ISSN 1027-4510, Journal of Surface Investigation: X-ray, Synchrotron and Neutron Techniques, 2023, Vol. 17, No. 2, pp. 352–356. © Pleiades Publishing, Ltd., 2023.
Russian Text © The Author(s), 2023, published in Poverkhnost', 2023, No. 3, pp. 40–45.

Effect of Ba^+-Ion Implantation on the Composition and Electronic Structure of Silicate Glasses

D. A. Tashmukhamedova[a], *, A. N. Urokov[a], G. Abdurakhmanov[b], and B. E. Umirzakov[a]

[a] *Tashkent State Technical University named after Islam Karimov, Tashkent, 100095 Uzbekistan*

[b] *National University of Uzbekistan named after Mirzo Ulugbek, Tashkent, 100174 Uzbekistan*

**e-mail: ftmet@mail.ru*

Received January 17, 2022; revised June 26, 2022; accepted June 26, 2022

Abstract—Effects of Ba^+-ion implantation into silicate glass and its after annealing on the composition, density of electronic states, and parameters of the energy bands are investigated by Auger electron, ultraviolet photoelectron, and light-absorption spectroscopic techniques. It is shown that nonstoichiometric oxides of Si, Pb, and Ba, as well as unbound atoms of the same elements, are formed in the ion implanted layer after ion implantation. As a result, there is a significant change in the electronic structure of silicate glass, in particular, the band gap decreases by ~2 eV. After annealing at $T = 1000$ K, unbound Si, Pb, and Ba atoms disappear in the ion implanted layer (within the limits of sensitivity of an Auger-electron spectrometer) and stoichiometric oxides such as SiO_2, PbO, and BaO are formed.

Keywords: silicate glass, ion implantation, ion dose, spectroscopy, band parameters, nanofilms, photon energy, ion etching, Auger spectrum, distribution profiles

DOI: 10.1134/S1027451023020180

INTRODUCTION

The overwhelming majority of silicates are good insulators. For instance, led silicate glass of the composition $2SiO_2 \cdot PbO$ has a resistivity exceeding 10^{16} Ohm · cm and a band gap of about 3.3 eV [1]. After implanting with transition metal (Cu, Fe, Mn, V, Ru, etc.) oxides the resistivity of silicate glass decreases to 10^{-2}–10^{-3} Ohm · cm [2] and the thermoelectric-power coefficient increases from ≈10 to 1700 μV/K [3–7].

We note that the implanting of silicate glass means a process similar to the implanting of semiconductors: the powder of glass synthesized at 1100–1500°C is mixed in the required proportion with powder of the implanting oxide (ligature) and again sintered but now at $T_f = 500$–950°C. At present, the composition and structure of the surface of the following silicate glasses have been well studied: 33 wt % SiO_2 + 67 wt % PbO (S71-K), 29 wt % SiO_2 + 67 wt % PbO + 4 wt % BaO (B34E).

Interest in studying implanted silicate glasses is, first of all, explained by their application for producing film resistors and chips in sensors for various physical and chemical impacts [8–10].

In [11], ideas about the pseudo-slit and nanocrystals are employed to explain the mechanism of the conductivity of silicate glass implanted with transition metal oxides (thick-film resistors). The pseudo-slit appears between the top of the valence band of glass and the impurity band generated by the diffusion of ligature atoms into the glass during sintering. Nanocrystals formed in glass during its preparation undergo structural transformations at high temperatures and act as centers of charge-carrier locations. Qualitative agreement is achieved between the model and the experimental temperature dependence of the conductivity of implanted glass in the range from 85 to 1100 K. We note that in all cases, silicate glasses were implanted during their synthesis; therefore, the implanting had a volumetric character.

The very first studies of the conductivity mechanism of thick-film resistors based on silicate glasses of different compositions were carried out for samples with ion implantation [12]. It was shown that the conductivity was not ionic and provided not by electron jumps. However, later, all studies of implanted silicate glasses [13–16] were carried out for samples implanted by the joint sintering of powders of silicate glasses with submicron particles and implanting metal oxide at temperatures about 1123 K. All researchers supposed that softened glass only bound ligature particles and conductivity was facilitated by electron hopping between these particles (Mott conductivity). Although in [17] and [18], by electron microprobe analysis it was revealed that Ru atoms from RuO_2 (main ligature) diffused into glass to a depth of about 1 μm; however, this fact was not taken into account in the consideration of conductivity mechanisms of implanted glass. Only in

[19] was it shown that glass and the ligature actively interacted during sintering, in particular, ligature atoms diffused into glass at a distance exceeding the diameter of glass particles. Therefore, the entire glass volume is implanted and becomes conductive. However, the state of ligature atoms in implanted glasses was not investigated in [19].

This work is devoted to the effect of implantation of Ba^+ ions with an energy of $E_0 = 1$ keV at high doses (at a saturation dose of $D = D_{sat} = 6 \times 10^{16}$ cm^{-2}) on the elemental and chemical compositions, the density of electron states of the valence band, and the parameters of the energy states of silicate glasses of the approximate composition 33 wt % SiO_2 + 67 wt % PbO.

EXPERIMENTAL

Samples of silicate glasses were prepared for the experiments from powders with particle sizes of 0.1–0.2 μm. They were obtained by grinding in agate drums of the XQM-0.4A TENCAN planetary mill. The mixture for preparing the glass consisted of VS-050-1 GOST (State Standard) 22551-2019 quartz sand (for preparing crystal glass) and other chemically pure oxides. Glass of the composition $2SiO_2 \cdot PbO$ was prepared in platinum crucibles at 1770 ± 10 K for 1 h; glasses of other compositions were prepared at 1620 ± 10 K for 1 h. Then glass powders were mixed with an organic ligature (10% solution of nitrocellulose in α-terpineol). The obtained paste was deposited through a mesh stencil on a ceramic substrate of 96% Al_2O_3 (M7), dried at 420 ± 10 K for 1 h, and sintered at 1123 ± 1 K for 10 min (total sintering time of 1 h). After sintering a continuous, homogeneous (verified by an optical microscope) glass layer with a thickness of 25 μm, a smooth surface, and a characteristic glass luster was formed on the substrate. This technology is typical of preparing thick film resistors with the only difference being that in the latter case, implanting metal oxide (often RuO_2 or bismuth and lead ruthenates) with particle sizes of 0.3–0.5 μm is added to the glass powder. The concentration of implanting metal oxide varies from 5 to 60 wt % depending on the required resistivity of the sample. The particle-size distribution of glass powders and implanting oxide was determined by a Photocor Mini laser analyzer with an error of 1%.

Ba^+ ions with energies ranging from 0.5 to 5 keV were implanted at a saturation dose of $D = D_{sat} = (6–8) \times 10^{16}$ cm^{-2}. Barium titanate (BaTi) pellets were the source of barium. During the heating of a quartz tube filled with BaTi pellets, barium vapor is formed. Part of it falling on the surface of the red-hot tungsten wire is ionized. The main studies were performed at an ion energy of $E_0 = 1$ keV. At $E_0 \geq 2$ keV the BaO compound did not form in the ion-implanted layer with good stoichiometry.

The studies were carried out using Auger electron and photoelectron spectroscopy and by measuring the intensity of light passing through the sample. The photon energy $h\nu$ was varied within 0.2–1.5 eV ($\lambda \approx$ 6200–800 nm). The atomic depth distribution profiles d were determined by Auger-electron spectroscopy in combination with the layer-by-layer etching of the surface by Ar^+ ions with an energy of $E_0 = 2$ keV at an angle of 5°–10° relative to the sample surface. The concentrations of silicate-glass components before and after ion implantation were determined with an error of 5–8 at %, and the determination error of the energy-band parameters was ~0.1 eV.

RESULTS AND DISCUSSION

The silicate glass was degassed before ion implantation by heating at $T = 1\,000$ K for 2–3 h in a vacuum chamber with a residual pressure of 10^{-6} Pa. Figure 1 depicts the Auger spectrum of the surface of the well-degassed silicate glass, implanted by Ba^+ ions with the energy $E_0 = 1$ keV at a dose $D = 6 \times 10^{16}$ cm^{-2} before and after annealing at $T = 1000$ K for 40 min. The spectrum of silicate glass mainly exhibits intense peaks corresponding to SiO_2 and PbO. Apart from these elements, low-intensity peaks of Mn, Cu, and Mg are detected. The total concentration of these elements does not exceed 2–3 at %; they are not taken into account in the calculations.

The estimated concentrations of SiO_2 and PbO oxides on the surface and in the bulk are listed in Table 1. The

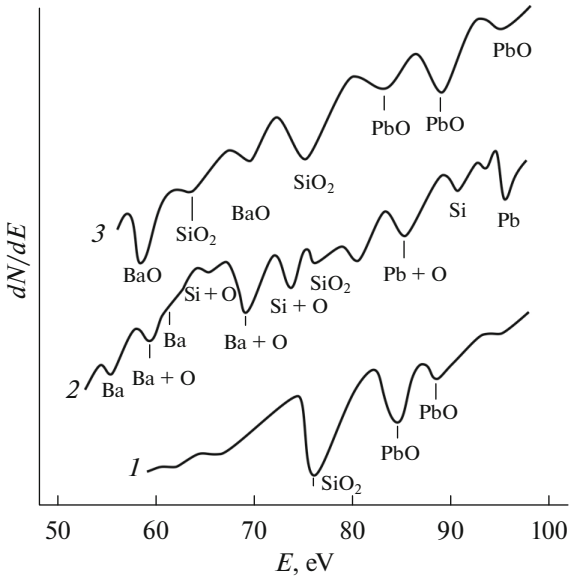

Fig. 1. Auger spectra of: well-degassed silicate glass (*1*); silicate glass after implantation by Ba^+ ions with $E_0 = 1$ keV at $D = 6 \times 10^{16}$ cm^{-2} (*2*); ion-implanted silicate glass after annealing at $T = 1000$ K (*3*).

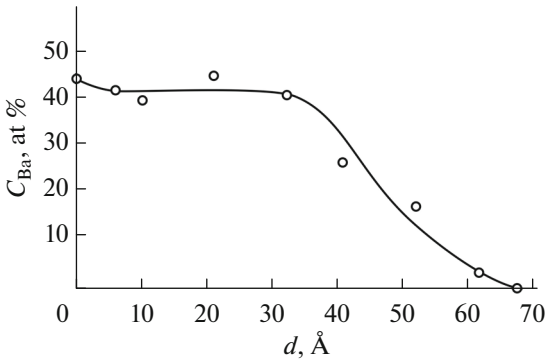

Fig. 2. Dependence of the Ba concentration on the sample depth for the glass sample implanted by Ba^+ ions with E_0 = 1 keV at the dose $D = 6 \times 10^{16}$ cm^{-2}.

data for the volume were borrowed from [1]. It is seen that the concentrations of oxides on the surface and in the bulk are different.

Upon Ba^+-ion bombardment with the energy E_0 = 1 keV, the composition and structure of the surface abruptly change (Fig. 1, curve *2*). The Ba concentration on the surface is ~40–45 at %. The majority of Ba ions (~80–85%) form compounds with oxygen, i.e., the surface composition dramatically changes. In particular, the intensity of Auger peaks corresponding to SiO_2 and PbO drastically decreases, peaks characteristic of nonstoichiometric Pb–O, Si–O, and Ba–O compounds appear along with peaks of unbound Pb, Si, and Ba atoms (Table 2). After annealing at T = 1000 K the Auger peaks corresponding to Ba, Si, and Pb atoms disappear and intense peaks of SiO_2, PbO, and BaO arise. Table 2 lists the estimated concentrations of oxides and free atoms before and after annealing ion-implanted silicate glasses at the optimal temperature (T = 1000 K). From Table 2 it is seen that after annealing ion-implanted silicate glass, the surface concentration of free Si, Pb, and Ba atoms decreases to zero. The concentrations of SiO_2 and PbO oxides noticeably increase while the concentration of the nonstoichiometric Ba–O compound decreases by 8–10 mol %. The intense desorption of Ba from ~25–30 Å thick ion-implanted layers seems to occur after annealing. These layers consist of SiO_2, PbO, and BaO oxides with stoichiometric composition good enough for the application in silicate glasses.

Table 1. Concentrations of oxides on the surface and in the bulk of glass

Object	C, wt %	
	SiO_2	PbO
On the surface	39	61
In the bulk [1]	33	67

Figure 2 depicts the distribution profiles of the total concentration of Ba atoms (C_{Ba}) in the glass bulk. It is seen that the Ba concentration barely changes up to a depth of 25–30 Å. It may be assumed that in the range d = 0–30 Å, the concentrations of other elements also do not change. At $d \geq 30$ Å C_{Ba} abruptly decreases, and at d = 70 Å it approaches zero.

Information was obtained on the density of state of valence electrons in the "pure" and ion-implanted silicate glasses. Figure 3 shows the energy-distribution curves of photoelectrons of "pure" and ion-implanted (by ions with an energy of E_0 = 0.5 keV, the dose was $D = 6 \times 10^{16}$ cm^{-2}) silicate glasses before and after annealing at T = 1000 K, which were measured upon 10.8 eV photon irradiation. To interpret the features (maxima) observed in the spectra, we preliminarily obtained the photoelectron spectra of relatively thick (thickness more than 200 Å) SiO_2, PbO, and BaO films. In the case of unimplanted glass, we assign the feature observed at $E_b = -1$ eV to surface states. The features at $E_b = -1.8$ and -5.2 eV correspond to SiO_2; the features at $E_b = -2.2$ and -3.3 eV correspond to PbO. The positions of the main maxima change after ion implantation, their intensities substantially decrease, and new features appear at $E_b = -0.3$ and -0.8 eV, which seem to be due to the excitation of electrons from Ba atoms and nonstoichiometric barium oxide. These changes are caused by the decomposition of Pb and Si oxides, the formation of nonstoichiometric Pb, Ba, and Si oxides, and the presence of unbound Ba, Pb, and Si atoms on the surface layers. After annealing the ion-implanted sample, its spectrum demonstrates pronounced maxima characteristic of BaO, SiO_2, and PbO. It is possible to find the top of the valence band E_V relative to the vacuum level from the photoelectron spectrum. It is equal to the photoelectron work function Φ:

$$E_V = \Phi = h\nu - \Delta E, \quad (1)$$

Table 2. Concentrations of nonstoichiometric oxides and Si, Pb, and Ba atoms (mol %) on the surface of silicate glass implanted by Ba^+ ions with the energy E_0 = 1 keV at $D = 6 \times 10^{16}$ cm^{-2} before and after annealing at T = 1000 K

Object	Si–O	Pb–O	Ba–O	Ba	Si	Pb
Before annealing	16	30	38	10	2	4
After annealing	28SiO_2	43PbO	29BaO	0	0	0

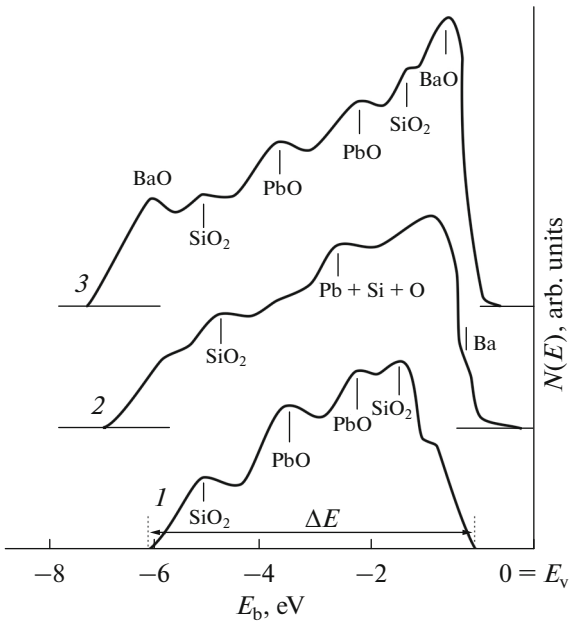

Fig. 3. Photoelectron energy distribution curves for: unimplanted glass (*1*); glass after Ba^+-ion implantation with $E_0 = 1$ keV at $D = 6 \times 10^{16}$ cm^{-2} (*2*); after annealing the ion-implanted sample at $T = 1000$ K (*3*).

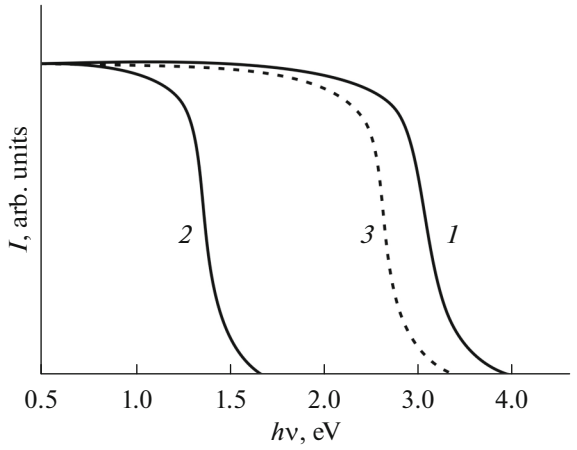

Fig. 4. Dependence of the passing light intensity on the photon energy for: unimplanted glass (*1*); glass after Ba^+-ion implantation with $E_0 = 1$ keV at $D = 6 \times 10^{16}$ cm^{-2} (*2*); after annealing the ion-implanted sample at $T = 1000$ K (*3*).

where ΔE is the width of the energy-spectrum curve. We note that the analysis of the intensity dependence of light passing through the sample enables the determination of the main band parameters of the materials under study.

Figure 4 presents the dependence of the intensity I of light passing through the sample on the photon energy for these systems. In all cases [20, 21], the I values do not significantly change with increasing $h\nu$ at first. When a certain photon energy is reached, I abruptly decreases almost to zero. Extrapolation of this part of the curve to the $h\nu$ axis gives an approximate value of the band gap E_g. The use of the known Φ and E_g values enables determination of the electron affinity χ by the formula

$$\chi = E_C = \Phi - E_g. \quad (2)$$

Table 3 lists the band energy parameters of the studied samples. It is seen that after Ba^+-ion implantation all energy-band parameters substantially change. In particular, the averaged E_g value decreases to ~2 eV (~2.5 times), which can be explained by the formation of nonstoichiometric Si–O, Pb–O, Ba–O oxides and the appearance of unbound Si, Pb, and Ba atoms in them. After annealing this system at $T = 1000$ K, an oxide film consisting of stoichiometric BaO, SiO_2, and PbO oxides is formed.

CONCLUSIONS

It is shown that the concentrations of oxides on the surface and in the bulk of silicate glass having the approximate composition of 33 wt % SiO_2 + 67 wt % PbO are significantly different. We found the optimal conditions for Ba^+-ion implantation and subsequent annealing to obtain a nanometer-thick film consisting of Ba, Si, and Pb oxides on the surface of silicate glass. The density of state of valence electrons is determined and the energy-band parameters are estimated for the samples under study. In particular, it is demonstrated that ion implantation causes a 2.5 times decrease in the band gap E_g of silicate glasses. The main mechanisms of changes in electron structures of the surfaces of silicate glasses during ion implantation and subsequent annealing are revealed.

Table 3. Band energy parameters of the studied samples of silicate glass: before ion irradiation, after Ba^+-ion irradiation with the energy $E_0 = 1$ keV, and after annealing Ba-ion implanted glass at $T = 1000$ K

Sample	Band parameters, eV		
	E_V, eV	E_g, eV	χ, eV
Before irradiation	5.2	3.4	1.8
After irradiation	4.35	1.45	2.9
After annealing	4.7	3.1	1.6

CONFLICT OF INTEREST

We declare that we have no conflict of interest.

REFERENCES

1. G. Abdurakhmanov, in *New Insights into Physical Science*, Vol. 4, Chapter 6: *Electrical Conduction in implanted Silicate Glasses (Thick Film Resistors)* (Book Publ. Int., London, 2020). https://www.doi.org/10.9734/bpi/nips/v4
2. G. Abdurakhmanov and N. G. Abdurakhmanova, Phys. Status Solidi A **202**, 1799 (2005). https://www.doi.org/10.1002/pssa.200420036
3. Y. Zheng, J. Atkinson, and R. Sion, J. Phys. D: Appl. Phys. **36**, 1153 (2003). https://www.doi.org/10.1088/0022-3727/36/9/314
4. C. Grimaldi, in *Printed Films*, Ed. by M. Prudenziati and J. Hormadaly (Cambridge, Woodhead, 2012), Chap. 5.
5. M. Moroz, Thick film systems for challenging applications, in *IMAPS SoCal'15 Tech. Symp.* (Santa Ana, CA, 2015).
6. K. Adachi and H. Kuno, Am. Ceram. Soc. **83**, 2441 (2000). https://www.doi.org/10.1111/j.1151-2916.2000.tb01574.x
7. K. S. R. C. Murthy, Int. J. Adv. Res. **7**, 238 (2019). https://www.doi.org/10.21474/IJAR01/8811
8. S. Bindu and M. S. Suresh, Br. J. Appl. Sci. Technol. **6**, 342 (2015).
9. M. Wen, X. Guan, H. Li, and J. Ou, Phys. A (Amsterdam, Neth.) 301, 111779 (2020). https://www.doi.org/10.1016/j.sna.2019.111779
10. G. Abdurakhmanov, V. I. Shimanski, B. L. Oksengendler, B. E. Umirzakov, and A. N. Urokov, Tech. Phys. **66**, 269 (2021). https://doi.org/10.1134/S106378422102002X
11. C. C. Sartain, W. D. Ryden, and A. W. Lawson, J. Non-Cryst. Solids **5**, 55 (1970). https://www.doi.org/10.1016/0022-3093(70)90196-1
12. *Printed Films: Materials Science and Applications in Sensors, Electronics and Photonics*, Ed. by M. Prudenziati and J. Hormadaly (Woodhead, Cambridge, 2012).
13. O. A. Gudaev and V. K. Malinovskii, Phys. Solid State **44**, 2219 (2002).
14. X. J. Zhao and J. Y. Zhao, Adv. Mater. Res. **472–475**, 1514 (2012). https://www.doi.org/10.4028/www.scientific.net/amr.472-475.1514
15. K. Flachbart, V. Pavlík, N. Tomašovičova, C. J. Adkins, M. Somora, J. Leib, and G. Eska, Phys. Status Solidi B **205**, 399 (1998).
16. D. K. C. MacDonald, *Thermoelectricity: An Introduction to the Principles* (Dover, Mineola, 2006).
17. K. Adachi, S. Iida, and K. Hayashi, J. Mater. Res. **9**, 1668 (1994). https://www.doi.org/10.1557/JMR.1994.1866
18. O. Abe and Y. Taketa, J. Phys. D: Appl. Phys. **24**, 1163 (1991). https://www.doi.org/10.1088/0022-3727/24/7/022
19. G. Abdurakhmanov, G. S. Vakhidova, and L. Tursunov, World J. Condens. Matter Phys. **1**, 1 (2011). https://www.doi.org/10.4236/wjcmp.2011.11001
20. E. S. Ergashov, D. A. Tashmukhamedova, and E. Rabbimov, J. Surf. Invest.: X-ray, Synchrotron Neutron Tech. **9**, 350 (2015). https://doi.org/10.1134/S1027451015020287
21. E. S. Ergashov, D. A. Tashmukhamedova, and B. E. Umirzakov, J. Surf. Invest.: X-ray, Synchrotron Neutron Tech. **11**, 480 (2017). https://doi.org/10.1134/S1027451017020252

Translated by L. Chernikova